

Electrical characterization to 4 THz of *N*- and *P*-type GaAs using THz time-domain spectroscopy

N. Katzenellenbogen and D. Grischkowsky

IBM Watson Research Center, P.O. Box 218, Yorktown Heights, New York 10598

(Received 28 February 1992; accepted for publication 2 June 1992)

Using a high-performance optoelectronic THz beam system for time-domain spectroscopy, we have measured the absorption and index of refraction of *N*- and *P*-type doped GaAs from low frequencies to 4 THz. From these measurements the complex conductance was obtained over the same frequency range. All of the results were well fit by Drude theory.

In contrast to silicon, it is not possible to electrically characterize GaAs wafers with simple mechanical contacts, due to the Schottky barrier at the metal/GaAs interface. For such characterization ohmic contacts must be fabricated on the wafer itself. Accordingly, manufacturers specifications on device-grade GaAs wafers are relatively imprecise. This is especially true for *N*-type doping, due to the lower concentrations required. Therefore, a contactless method of electrical characterization of GaAs wafers would be extremely desirable. Previous work has proposed and demonstrated that far-infrared spectroscopy is a possible solution.¹ Pioneering far-infrared absorption measurements have been made on *N*-type GaAs at several different free carrier concentrations.² The measured absorption due to the free carriers agreed with Drude theory on the high-frequency wing and allowed for an "optical" determination of the free carrier density and mobility. However, the peak absorptions measured were only a fraction of that expected from Drude theory. Later measurements with discrete far-infrared laser sources showed that these early measurements were severely compromised by scattered far-infrared light, which placed a limit on the magnitude of the absorption that could be measured.³

The key parameters characterizing the dynamics of free carriers in semiconductors are the plasma frequency ω_p and the carrier damping rate $\Gamma = 1/\tau$, where τ is the carrier collision time. Because ω_p and Γ characteristically have THz values, measurements spanning the values of these parameters must be performed in the difficult THz frequency range.⁴ The experiments described in this letter present such measurements on device-grade, *N*-type and *P*-type GaAs wafers, by the newly developed THz time-domain spectroscopy (TDS) technique.^{4,5} Our results show, for the first time, the absorption and index of refraction due to the free carriers in GaAs measured over the peaks of their response and extending from low frequencies to beyond 4 THz. The fact that the measured frequency-dependent absorption and index of refraction are mostly due to the free carriers allows the complex conductivity to be determined from the measurements over the full frequency range. The results are fit to surprising accuracy by the Drude theory.

The THz-TDS measurements were performed by measuring freely propagating, THz electromagnetic pulses

transmitted through the GaAs wafer under investigation. These transmitted pulses were then compared to the measured THz pulses with no sample in place. Analysis of the respective numerical Fourier transforms determines the frequency dependent absorption and index of refraction.⁵ The 40-mm-diameter wafers were obtained from Sumitomo Electric, with the *P* type specified to be between 0.52 and 0.56 Ω cm with a zinc dopant, and the *N* type to be between 0.1 and 1 Ω cm with a silicon dopant. Because of the large absorptions, the *P*-type and *N*-type wafers were thinned to 230 and 190 μ m, respectively.

Earlier THz-TDS measurements on doped silicon wafers were limited to the highest frequency of 2 THz.⁴ Since then, the frequency range of the optoelectronic THz beam system, illustrated schematically in Fig. 1(a), has been extended by combining a new type transmitter⁶ with a high-performance SOS receiver.⁷ As shown in Fig. 1(b), this system can now generate and measure femtosecond pulses of freely propagating THz radiation with a signal-to-noise ratio of better than 1000. An expanded view of this input pulse [Fig. 1(b)] for the *N*-type measurements is presented in Fig. 1(c), where on the trailing edge rise and fall times faster than 160 fs can be observed. These values are consistent with the receiver response time of 150 fs.⁷ The amplitude spectrum shown in Fig. 1(d) extends from low frequencies to 5 THz and is obtained by a numerical Fourier transform of the measured pulse of Fig. 1(b).

Our THz-TDS measurements of the exceptionally high absorption of the *N*-type GaAs sample are shown in Fig. 2(a) along with previous Fourier-transform-spectroscopy (FTS) measurements on a sample with an equivalent dopant concentration (triangles)² and discrete measurements on the same sample with far-infrared laser lines (squares).³ As determined by a Drude theory fit, our sample has a free carrier concentration of $N_e = 7.8 \times 10^{15}/\text{cm}^3$, while for the sample of the earlier works,^{2,3} $N_e = 7.1 \times 10^{15}/\text{cm}^3$. Surprisingly, where the absorption is high, these measurements on similar samples show quite different results. However, the measurements converge at the highest frequencies where the absorption is relatively low. As discussed in Ref. 3, we consider this to be mainly due to the sensitivity of the FTS measurements to scattered far-infrared light. Compared to the previous techniques which measure power, an advantage of THz time-domain spectroscopy is that it is a coher-

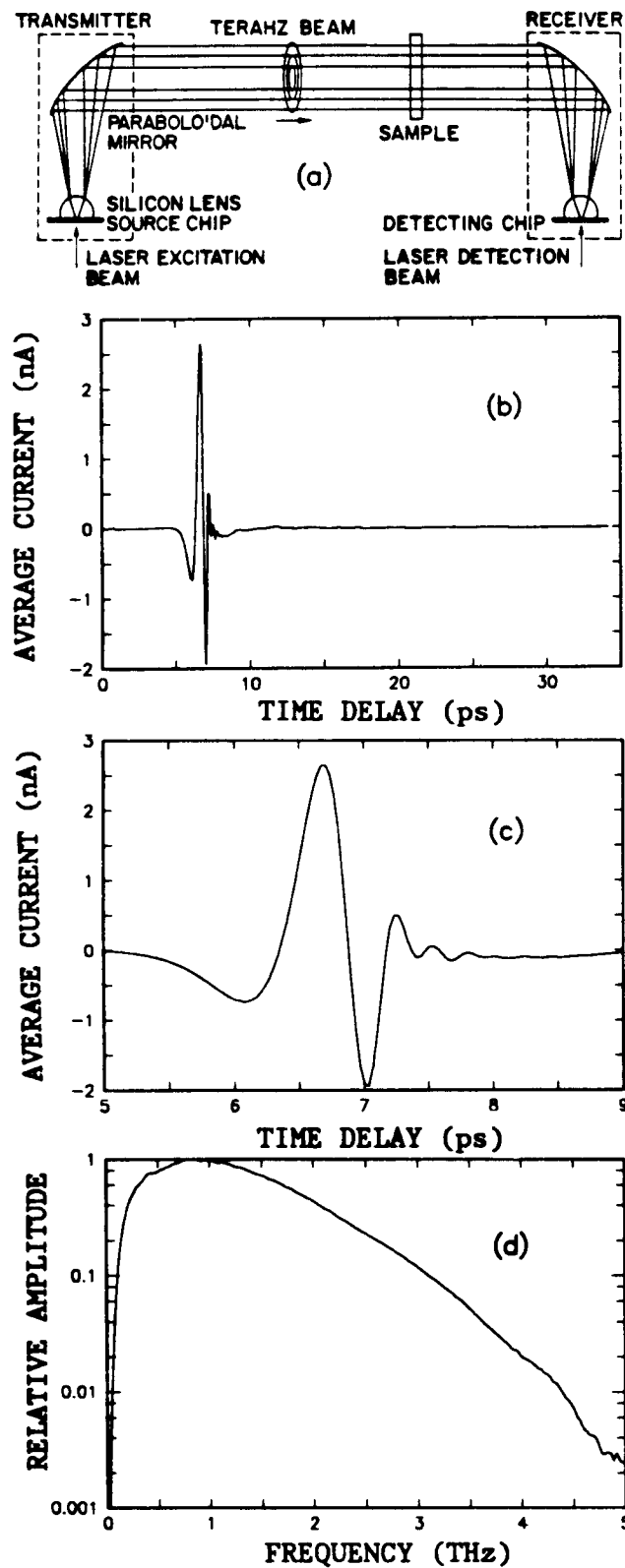


FIG. 1. (a) The optoelectronic THz beam system. (b) Measured transmitted THz pulse without sample. (c) Expanded view of measured THz pulse without sample. (d) Amplitude spectrum of (b).

ent technique that measures the amplitude of the propagating field. The system described by Fig. 1 has a dynamic range of better than 500 on the peak amplitude of the numerical Fourier transform of the measured pulse. With

this system it is possible to obtain a power spectrum with a dynamic range of 250 000. This feature, combined with the fact that the THz beams are highly directional and allow for good shielding from scattered THz radiation, makes possible such measurements of high absorptions.

The frequency-dependent complex dielectric constant ϵ is equal to the square of the complex index of refraction $n = n_r + in_i$. The imaginary index n_i is determined by measuring the power absorption coefficient $\alpha = n_i 4\pi/\lambda_0$. The doped GaAs sample's dielectric response is described by the following general relationship, independent of the functional form of the conductivity:

$$\epsilon = \epsilon_{\text{GaAs}} + i\sigma/(\omega\epsilon_0), \quad (1)$$

where ϵ_{GaAs} is the frequency-dependent dielectric constant of undoped GaAs, σ is the complex conductivity, and ϵ_0 is the free-space permittivity. The complex conductivity of the Drude model is given by⁴

$$\sigma = i\epsilon_0\omega_p^2/(\omega + i\Gamma). \quad (2)$$

As can be seen in Fig. 2(a), from low frequencies up to 4 THz, the *N*-type absorption measurements (dots) are well described by the absorption calculated from n_i using Eq. (1) and σ of the Drude model Eq. (2). The fit is better than that obtained for more lightly doped *N*-type silicon in the more limited frequency range up to 2 THz.⁴ Even though the etalon resonances were numerically removed from the data, there are still some remaining etalon oscillatory effects at the highest frequencies. It is important to note that because of the exceptionally large absorption, the transmission is complex, thereby causing an additional significant phase shift. Compared to the measured absorptions for both the *N*- and *P*-type samples, the absorption of the undoped GaAs host crystal is negligible.^{2,5} For the *P*-type absorption results (circles) Drude theory fits the measurements up to 2 THz, but thereafter the measured absorption continues to increase relative to the Drude value. It is not clear whether the additional absorption is due to the electrical response of the free carriers and thereby is a deviation from the theory or is simply the GaAs absorption, increased by the presence of the dopant. For the *N*-type sample the Drude theory parameters are $\omega_p = 2\pi \times (3.00 \text{ THz})$ and $\Gamma = 2\pi \times (0.96 \text{ THz})$, corresponding to $\tau = 165 \text{ fs}$, while for the *P* type the best fit is obtained with $\omega_p = 2\pi \times (3.79 \text{ THz})$ and $\Gamma = 2\pi \times (2.86 \text{ THz})$, corresponding to $\tau = 56 \text{ fs}$. For both samples the calculation utilized the undoped GaAs index of refraction $n_r = 3.59 + 0.005 f^2$, where f is the frequency in THz.⁵

The measured index of refraction is shown in Fig. 2(b) for both the *N*- and *P*-type samples. The fit to Drude theory at the lower frequencies is quite good. Well resolved minima are observed, and the large changes in the index agree with theory. The fact that the index of refraction fits well over the entire range implies that the additional *P*-type absorption is not due to the electrical response of the free carriers.

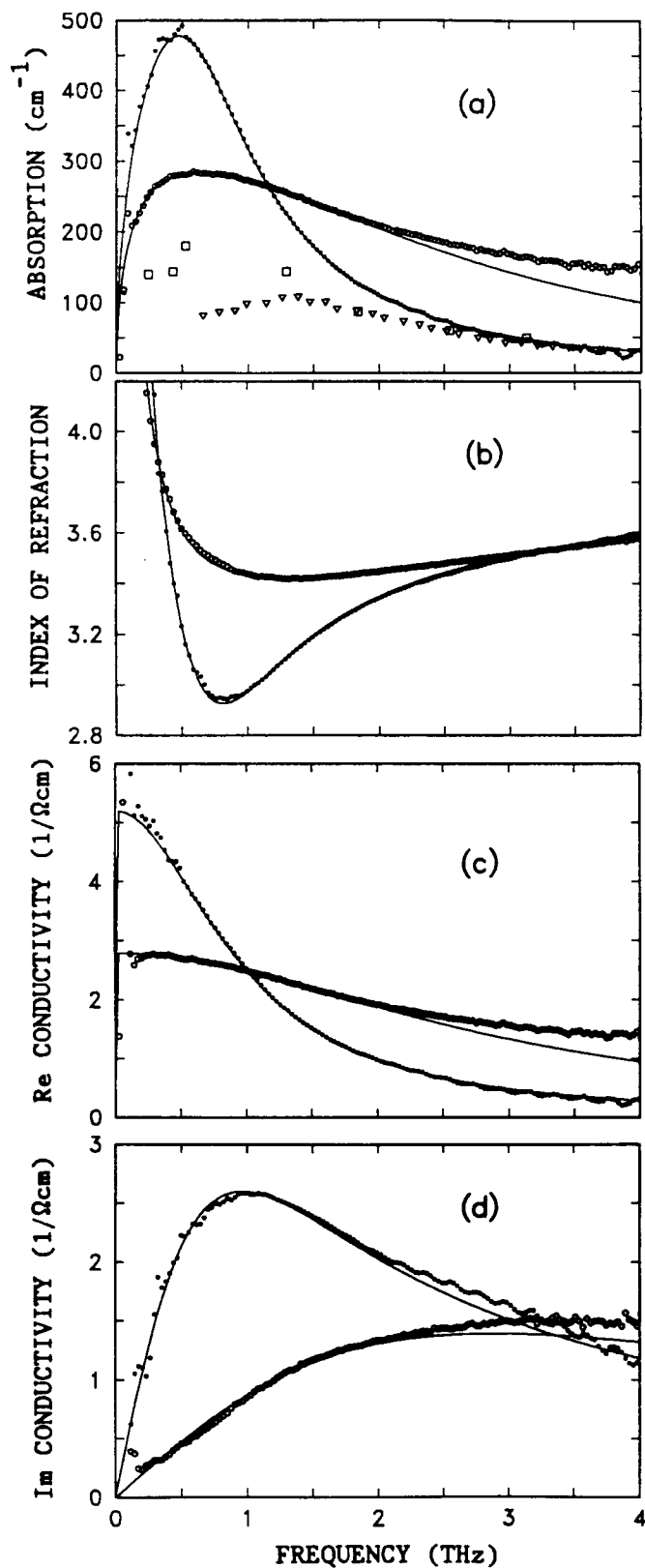


FIG. 2. Theory (solid lines) and measurements for 0.19 Ω cm *N*-type (dots) and 0.36 Ω cm *P*-type (circles) GaAs at room temperature. (a) Power absorption coefficient. Our measurements (dots and circles). Earlier measurements on *N*-type GaAs of Ref. 2 (triangles) and of Ref. 3 (squares). (b) Index of refraction. (c) Real part of the conductivity. (d) Imaginary part of the conductivity.

Given the measured absorption and index of refraction [Figs. 2(a) and 2(b)] and the absorption and index of refraction of undoped GaAs,^{2,5} the general relationship of Eq. (1) determines the real σ_r and imaginary σ_i parts of the conductivity shown in Figs. 2(c) and 2(d). The conductive response extends to beyond 4 THz and shows an important crossover of the two curves.

From Eq. (2) for the *N*-type sample, $\sigma_r = 5.2/(\Omega \text{ cm})$ at dc, corresponding to a resistivity of 0.19 $\Omega \text{ cm}$, compared to a directly measured value of 0.14 $\Omega \text{ cm}$ and to the band between 0.1 and 1 $\Omega \text{ cm}$ specified by the manufacturer. For the *P*-type sample $\sigma_r = 2.8/(\Omega \text{ cm})$, corresponding to a resistivity of 0.36 $\Omega \text{ cm}$, compared to a directly measured value of 0.43 $\Omega \text{ cm}$ and to the manufacturer's specification of between 0.52 and 0.56 $\Omega \text{ cm}$. Given the effective masses $m_e = 0.067 m_0$ and $m_h = 0.34 m_0$, for the electrons and holes, respectively, the mobilities are calculated from the relationship $\mu = e/m^* \Gamma$ to be $\mu_e = 4300 \text{ cm}^2/\text{V s}$ and $\mu_h = 290 \text{ cm}^2/\text{V s}$, compared to Hall measurements of $\mu_e = 4300 \text{ cm}^2/\text{V s}$ and $\mu_h = 240 \text{ cm}^2/\text{V s}$. The mobility for our *N*-type sample was not specified, but for a more lightly doped sample with $N_e = 1 \times 10^{13}$, $\mu_e = 5700 \text{ cm}^2/\text{V s}$ was specified. For our *P*-type sample $\mu_p = 230 \text{ cm}^2/\text{V s}$ was specified, significantly lower than our measured value but in reasonable agreement with the Hall measurement. The THz-TDS experiments on doped silicon⁴ also measured mobilities significantly higher than the specified values. Using the relationship $\omega_p^2 = Ne^2/\epsilon_0 m^*$, the number density of free carriers N is obtained as $N_e = 7.8 \times 10^{15}/\text{cm}^3$ and $N_h = 5.7 \times 10^{16}/\text{cm}^3$. In summary, the precision of the absorption and index of refraction measurements determines the Drude fitting parameters to $\pm 2\%$ for ω_p and $\pm 5\%$ for Γ , and thereby device-grade GaAs wafers can be characterized by noncontact THz-TDS to high precision.

We acknowledge the excellent masks, wafer fabrication, and sample wafer thinning by Hoi Chan. Thomas Jackson and Stephen E. Ralph provided helpful comments on the manuscript. In addition, Thomas Jackson suggested and encouraged the use of his laboratory to make the Hall measurements.

¹J. F. Black, E. Lanning, and S. Perkowitz, *Infrared Phys.* **10**, 125 (1970).

²S. Perkowitz, *J. Phys. Chem. Solids* **32**, 2267 (1971).

³B. L. Bean and S. Perkowitz, *J. Opt. Soc. Am.* **67**, 911 (1977).

⁴M. van Exter and D. Grischkowsky, *Appl. Phys. Lett.* **56**, 1694 (1990); *Phys. Rev. B* **41**, 12 140 (1990).

⁵D. Grischkowsky, S. Keiding, M. van Exter, and Ch. Fattinger, *J. Opt. Soc. Am. B* **7**, 2006 (1990).

⁶N. Katzenellenbogen and D. Grischkowsky, *Appl. Phys. Lett.* **58**, 222 (1991).

⁷D. Grischkowsky and N. Katzenellenbogen, in *Proceedings of the Conference on Picosecond Electronics and Optoelectronics*, edited by T. C. L. Gerhard Sollner and Jagdeep Shah (Optical Society of America, Washington, D.C., 1991), Vol. 9, pp. 9-14.